

## Nonequilibrium fluctuation theory on pitting dissolution. III. Experimental examinations on critical fluctuation and its growth process in nickel dissolution

Miki Asanuma and Ryoichi Aogaki

Citation: [The Journal of Chemical Physics](#) **106**, 9944 (1997); doi: 10.1063/1.473881

View online: <http://dx.doi.org/10.1063/1.473881>

View Table of Contents: <http://scitation.aip.org/content/aip/journal/jcp/106/23?ver=pdfcov>

Published by the [AIP Publishing](#)

---

### Articles you may be interested in

[Atomic force microscopy study of oscillatory surface roughening in anodic dissolution of sputter-deposited nickel films](#)

J. Chem. Phys. **113**, 2397 (2000); 10.1063/1.482054

[Nonequilibrium fluctuation theory on pitting dissolution. II. Determination of surface coverage of nickel passive film](#)

J. Chem. Phys. **106**, 9938 (1997); 10.1063/1.473880

[Nonequilibrium fluctuation theory on pitting dissolution. I. Derivation of dissolution current equations](#)

J. Chem. Phys. **106**, 9930 (1997); 10.1063/1.473879

[Nonequilibrium fluctuation theory in electrochemical nucleation. III. Experimental determination of fluctuation growth rate in silver nucleation onto platinum electrode](#)

J. Chem. Phys. **106**, 6146 (1997); 10.1063/1.473236

[Nonequilibrium fluctuation theory in electrochemical nucleation. II. Experimental determination of critical fluctuation in silver nucleation onto platinum electrode](#)

J. Chem. Phys. **106**, 6138 (1997); 10.1063/1.473235

---



# Nonequilibrium fluctuation theory on pitting dissolution. III. Experimental examinations on critical fluctuation and its growth process in nickel dissolution

Miki Asanuma<sup>a)</sup> and Ryoichi Aogaki<sup>b)</sup>

Department of Product Design, Polytechnic University, 4-1-1, Hashimoto-dai, Sagamihara, 229-11, Japan

(Received 9 October 1996; accepted 12 March 1997)

Following part II, current–time transient in nickel pitting dissolution has been examined. After the passive film is broken, the resultant diffusion current decreases to the minimum value. The minimum current, as shown in part I, gives the ratio of the average critical concentration fluctuation on the completely active surface to its autocorrelation distance. Therefore, using the experimental data of the minimum current mentioned above and the average concentration fluctuation obtained in part II, the critical autocorrelation distance has been calculated. Since, in the stable region, the fluctuation is suppressed to maintain that the electrode surface is flat and stable, the autocorrelation distance tends to approach infinity. Therefore, the distance at the critical state is expected to be extraordinarily large; the value of about 1 mm has been actually obtained. This value is regarded to have some generality independent of the characteristics of the reaction because it is purely determined by the thermal motion of the solution particles. In fact, it is approximately agreeable with the value obtained for silver nucleation. Then, the fluctuations start unstable growth. As shown in part I, reflecting the fact that the instability arises from the electrostatic interaction of the solution particles in the electric double layer, the growth current substantially depends on the concentration of the supporting electrolyte and the externally applied electrode potential. © 1997 American Institute of Physics. [S0021-9606(97)51523-6]

## I. INTRODUCTION

Following passivity breakdown, the dissolution of a substrate metal induces pit formation. However, according to Sato,<sup>1</sup> such breakdown does not necessarily produce pits, that is, the primary factor determining the stability of pitting is the local ion buildup at film breakdown sites.<sup>2–5</sup> The mechanisms of the resultant dissolution are summarized as<sup>6</sup> (1) an aquoligand mechanism, (2) hydroxoligand mechanism, and (3) Anionoligand mechanism. Namely, pitting dissolution is controlled by the adsorption state of ions in the electrical double layer. Then, according to the change of the adsorption state, the substrate of the individual pit dissolves at a different rate, which suggests that pitting corrosion is essentially a heterogeneous reaction. Therefore, as mentioned in part I,<sup>7</sup> the dissolution current observed must be formulated not only by introducing the heterogeneity, but also by including the adsorption effect of ions.

For this purpose, the nonequilibrium fluctuations presented in a previous paper<sup>8</sup> are thought to be quite attractive since they inevitably include both the heterogeneity of the reaction and the adsorption effect of the ions; actually, they allow us to analyze the transient phenomena in the pitting dissolution.

In the theoretical calculation of the dissolution current, the autocorrelation distance of the asymmetrical nonequilibrium fluctuation is employed as the parameter to describe the heterogeneity. The adsorption effect is then introduced

through the critical condition for instability; the intense specific adsorption of anions makes the asymmetrical fluctuation unstable, so that the pitting dissolution progresses rapidly.

In this paper, for nickel pitting dissolution in NaCl solution, we first determine the function form of the autocorrelation distance by means of the theoretical prediction treated in part I. Then, the pit-growth current observed is compared with the theoretical equation derived in consideration of the unstable growth of the asymmetrical fluctuation. That is, the current must be expressed as an exponential function of the second order of time. The time coefficient of the function, i.e., the growth factor determines the rising rate of the current, which is related to the solution composition and the overpotential of the double layer.

## II. EXPERIMENT

The experiment was performed for nickel dissolution in the  $\text{NiCl}_2 + \text{NaCl}$  solution. The cell used and experimental procedures are the same as has been already explained in part II.<sup>9</sup>

## III. RESULTS AND DISCUSSION

### A. Determination of critical parameters

As mentioned in part II, applying an anodic potential step to the nickel electrode in NaCl solution, we initially observe diffusion current, which follows the double-layer charging current. As the initial diffusion current flows, the diffusion layer develops into the bulk of the solution. When the diffusion layer thickness increases much more than the autocorrelation distance of the asymmetrical nonequilibrium

<sup>a)</sup>Present address: Polytechnic Center Kanto, 78, Minami-Kibougaoka, Ashahi-ku, Yokohama, 241, Japan.

<sup>b)</sup>Electronic mail: aogaki@uitech.ac.jp

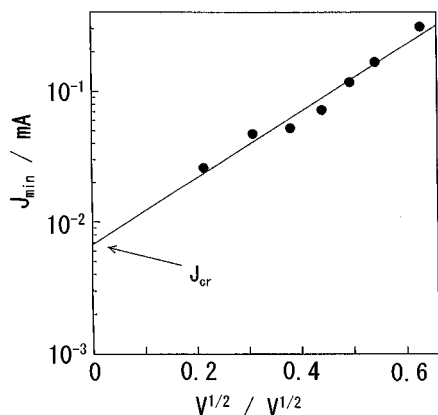


FIG. 1. Semilog plot of the minimum current,  $J_{\min}$  vs  $V^{1/2}$ .  $[\text{NaCl}] = 50 \text{ mol m}^{-3}$ ,  $[\text{NiCl}_2] = 0.1 \text{ mol m}^{-3}$ , and  $T = 300 \text{ K}$ .

fluctuation, as discussed in part I,<sup>7</sup> a steady state emerges, which corresponds to the minimum state of the current. According to part I, assuming the total double-layer overpotential  $\langle \Phi_0 \rangle \approx V$ , it can be expressed in the following form:

$$J_{\min} = J_{\text{cr}} \exp(B|V|^p), \quad (1)$$

where  $B$  and  $p$  are coefficients,  $V$  is the step potential measured from the critical potential, and  $J_{\text{cr}}$  means the pitting current at the critical potential, which is, in terms of the critical concentration gradient  $\alpha_{\text{cr}}$ , given by

$$J_{\text{cr}} = z_m F D_m S \alpha_{\text{cr}}, \quad (2)$$

where  $z_m$  and  $D_m$  are the charge number and diffusion coefficient of the dissolved metal ion, respectively.  $F$  is the Faraday constant, and  $S$  is the effective electrode area.

Moreover, with the average critical concentration fluctuation  $\tilde{c}_{\text{cr}}$  on the completely active surface and its autocorrelation distance  $\tilde{a}_{\text{cr}}$ ,  $\alpha_{\text{cr}}$  is written by

$$\alpha_{\text{cr}} = \frac{\tilde{c}_{\text{cr}}}{\tilde{a}_{\text{cr}}} \quad (3)$$

In Eq. (1), it is thought that  $p$  is a constant and  $B$  is a function of the coverage  $\theta$  of the passive film. Figure 1 shows a typical example of the plot of  $\log J_{\min}$  versus  $|V|^{1/2}$ , which has a good linear relation. After many examinations of the same kind,

$$p = \frac{1}{2}, \quad (4)$$

was experimentally determined. According to Eq. (1), the extrapolation of this plot to  $V = 0 \text{ V}$  gives  $J_{\text{cr}}$  value. Figure 2 shows that  $J_{\text{cr}}$  is independent of the  $\text{Ni}^{2+}$  ionic concentration. Similarly, as shown in Fig. 3, it is also irrespective of NaCl concentration. As mentioned in part II, the average critical concentration fluctuation  $\tilde{c}_{\text{cr}}$  on the complete active surface does not depend on the composition of the solution, having a constant value

$$\tilde{c}_{\text{cr}} = 1.32 \pm 0.11 \text{ mol m}^{-3}. \quad (5)$$

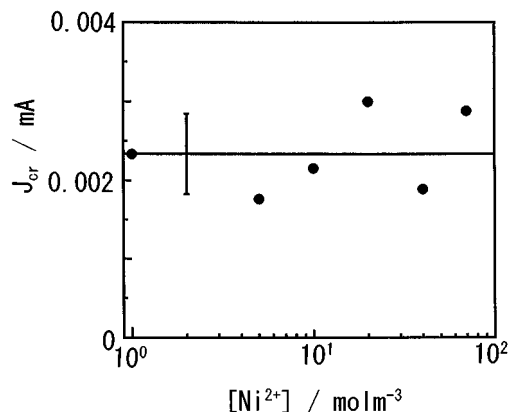


FIG. 2. Dependence of the critical current on  $\text{Ni}^{2+}$  ionic concentration.  $[\text{NaCl}] = 1000 \text{ mol m}^{-3}$ , and  $T = 300 \text{ K}$ .

This is quite different from the experimental result in the nucleation of silver onto a platinum electrode,<sup>10</sup> where  $\tilde{c}_{\text{cr}}$  depends on the solution composition. In the present case, the concentration fluctuation is provided by the dissolution of the substrate metal itself, without any supply from the solution phase, which reasonably supports the fact that  $\tilde{c}_{\text{cr}}$  is independent of the solution composition. This result also suggests that the resultant statistical parameter, i.e., the autocorrelation distance,  $\tilde{a}_{\text{cr}}$  is also indifferent of any of the ion and salt concentrations. Using Eqs. (2), (3), and (5) with the data obtained in Figs. 2 and 3,  $\tilde{a}_{\text{cr}}$  can be calculated; as exhibited in Figs. 4 and 5, the  $\tilde{a}_{\text{cr}}$  remains constant for  $\text{Ni}^{2+}$  ionic concentration and NaCl concentration. From the data, an extraordinarily large value in comparison with the scale of the fluctuation,

$$\tilde{a}_{\text{cr}} = 1.02 \pm 0.21 \text{ mm}, \quad (6)$$

is determined.

The reason why such a large value is obtained can be elucidated as follows: since in the stable region, all the fluctuations are decayed to zero to maintain that the electrode surface is flat and stable, the autocorrelation distance tends to approach infinity. To the contrary, in the unstable region,

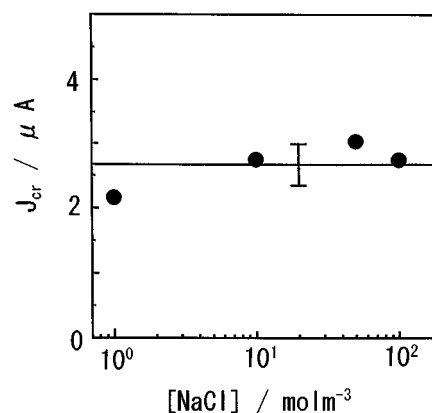


FIG. 3. Dependence of the critical current on NaCl concentration.  $[\text{NiCl}_2] = 0.1 \text{ mol m}^{-3}$ , and  $T = 300 \text{ K}$ .

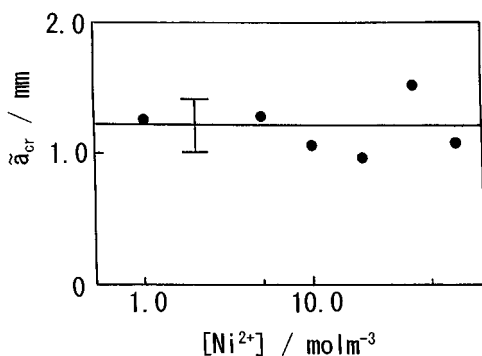


FIG. 4. Critical autocorrelation distance of nonequilibrium fluctuation on the completely active surface without any passive film against  $\text{Ni}^{2+}$  ionic concentration.  $[\text{NaCl}] = 1000 \text{ mol m}^{-3}$ , and  $T = 300 \text{ K}$ .

many new fluctuations grow up, so that the autocorrelation distance will take a small value. At the critical state, i.e., the boundary between the two regions, therefore, the fluctuation with an extraordinarily large autocorrelation distance appears, of which the value is regarded to have a generality independent of the characteristics of the reaction because it is purely determined by the coupling of the nonequilibrium fluctuation and the thermal motion of the solution particles. In fact, it is approximately in good agreement with the value,  $0.782 \text{ mm}$  obtained for silver nucleation onto the platinum electrode at the same temperature.<sup>10</sup> The fact that both values of  $\tilde{a}_{\text{cr}}$  in different reactions, even if approximately, coincide with each other reinforces the prediction that in the critical state, it is determined not by the individual nature of the electrode system but by the general nature of the thermal motion of the solution particles.

On the other hand, we can decide the  $B$  value in Eq. (1) from the slope of the plot in Fig. 1. As shown in Fig. 6, the values obtained are kept constant against the change of  $\text{Ni}^{2+}$  ionic concentration. However, in Fig. 7, they increase with increasing  $\text{NaCl}$  concentration. From the foregoing paper,<sup>9</sup> the coverage  $\theta$  of the passive film is known as a function of  $\text{NaCl}$  concentration, so that the present experi-

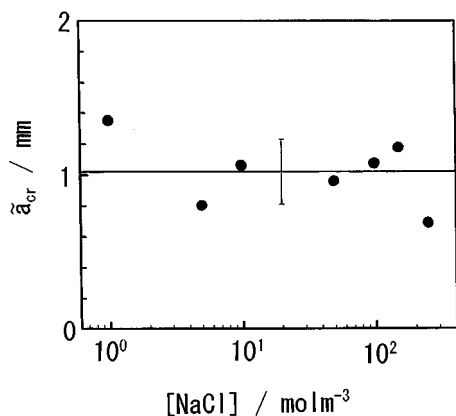


FIG. 5. Critical autocorrelation distance of nonequilibrium fluctuation on the completely active surface without any passive film against  $\text{NaCl}$  concentration.  $[\text{NiCl}_2] = 0.1 \text{ mol m}^{-3}$ , and  $T = 300 \text{ K}$ .

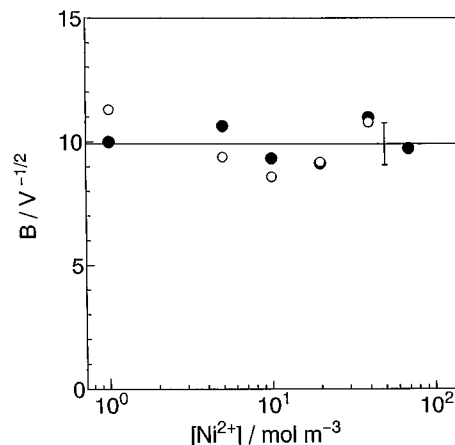


FIG. 6. Dependence of  $B$  values given by the minimum current  $J_{\text{min}}$  and the unstable component  $J_0$  of the minimum current on  $\text{Ni}^{2+}$  ionic concentration.  $[\text{NaCl}] = 1000 \text{ mol m}^{-3}$ , and  $T = 300 \text{ K}$ . ●;  $B$  from  $J_{\text{min}}$ , and ○;  $B$  from  $J_0$ .

mental result indicates that the  $B$  value is a function of  $\theta$ , whose actual form will be experimentally determined in the later section of this paper.

## B. Examination of pit-growth current

Asymmetrical nonequilibrium concentration fluctuations produced by the dissolution of the substrate metal gradually start to grow via the minimum current. Subsequently, the dissolution is accelerated according to the following equation:<sup>7</sup>

$$J = J_0 \exp(I_G t^2), \quad (7)$$

where  $J_0$  means the current component, which becomes unstable at the minimum state. Namely, only some of the fluctuations initially yielded can grow up with time. Therefore,  $J_0$  is expressed by introducing the instability ratio  $\gamma_u^a$  to the minimum current, as follows:

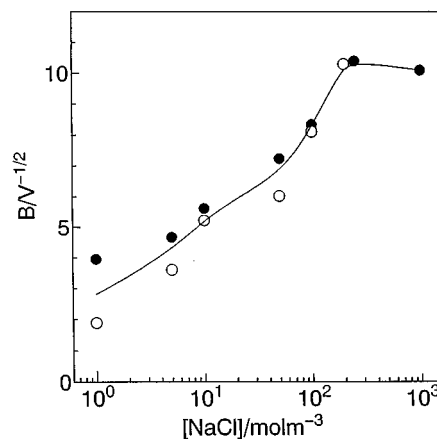


FIG. 7. Dependence of  $B$  values given by the minimum current  $J_{\text{min}}$  and the unstable component  $J_0$  of the minimum current on  $\text{NaCl}$  concentration.  $[\text{NiCl}_2] = 0.1 \text{ mol m}^{-3}$ , and  $T = 300 \text{ K}$ . ●;  $B$  from  $J_{\text{min}}$ , and ○;  $B$  from  $J_0$ .

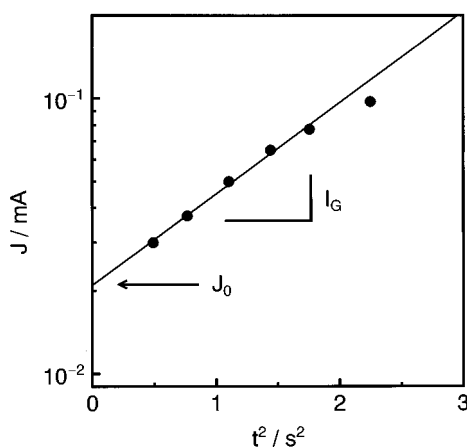


FIG. 8. Semilog plot of the pit-growth current,  $J$  vs  $t^2$ .  $V = 50$  mV,  $[\text{NiCl}_2] = 5 \text{ mol m}^{-3}$ ,  $[\text{NaCl}] = 1000 \text{ mol m}^{-3}$ , and  $T = 300$  K.

$$J_0 = \gamma_u^a J_{\min} \quad (8)$$

According to part I,<sup>7</sup>  $l_G$  is the growth factor of the pitting current, which is given by

$$l_G = \frac{1}{2} A_0^2 \alpha_{\text{cr}}^2 C_s^*(z = \infty) |V|^2 \exp(2B|V|^{1/2}), \quad (9)$$

where  $A_0$  is a constant, and  $C_s^*(z = \infty)$  is the NaCl concentration. Taking logarithms of the both sides of Eq. (7), it follows that

$$\log|J| = l_G t^2 + \log|J_0|. \quad (10)$$

Thus, as shown in Fig. 8, in plotting  $\log|J|$  versus  $t^2$ ,  $J_0$  and  $l_G$  are obtained from the intercept to the ordinate and the slope of the plot, respectively. From Eqs. (1) and (8),  $J_0$  is derived as

$$J_0 = J_0^{\text{cr}} \exp(B|V|^p), \quad (11)$$

where  $J_0^{\text{cr}}$  is the unstable component of the critical current  $J_{\text{cr}}$ .  $J_0$  in Eq. (11) has the same function of  $B$  and  $V$  as Eq. (1). Therefore, the instability ratio  $\gamma_u^a$  is defined as

$$\gamma_u^a = J_0^{\text{cr}} / J_{\text{cr}}. \quad (12)$$

In order to experimentally ascertain Eq. (11), according to Eq. (4), the plot of  $\log|J_0|$  versus  $|V|^{1/2}$  was performed in Fig. 9; a good linear relation was revealed. Then, we continued the same plots with changing the composition of the solution, so that  $J_0^{\text{cr}}$  from the intercept of the ordinate and  $B$  from the slope were decided. Figure 10 represents the dependence of  $J_0^{\text{cr}}$  on the  $\text{Ni}^{2+}$  ionic concentration, which remains constant. As mentioned before, in Fig. 2,  $J_{\text{cr}}$  has already been shown to be constant against  $\text{Ni}^{2+}$  ionic concentration; this means that the instability ratio  $\gamma_u^a$  is kept constant, being irrespective of the composition of the solution. According to Eq. (12), some experimental results of  $\gamma_u^a$  are shown in Fig. 11. From these data,

$$\gamma_u^a = 0.81 \pm 0.11, \quad (13)$$

is obtained. As a result, it can be said that about 80% of the total fluctuations that exist in the critical state become un-

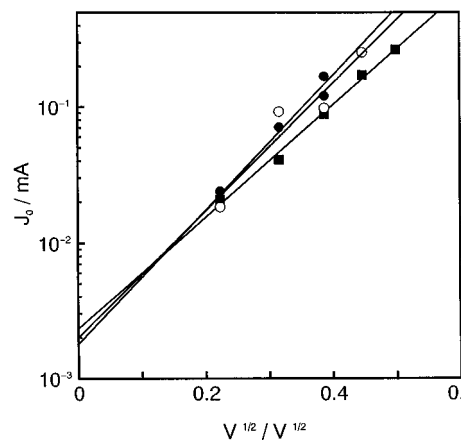


FIG. 9. Semilog plot of the unstable component  $J_0$  of the minimum current vs  $V^{1/2}$ .  $[\text{NaCl}] = 1000 \text{ mol m}^{-3}$ , and  $T = 300$  K.  $[\text{Ni}^{2+}]$ :  $\bullet$ ;  $1 \text{ mol m}^{-3}$ ,  $\blacksquare$ ;  $5 \text{ mol m}^{-3}$ , and  $\circ$ ;  $40 \text{ mol m}^{-3}$ .

stable. Here, the  $B$  values can be obtained from two different currents, i.e., the minimum current  $J_{\min}$  given by Eq. (1), and the unstable component  $J_0$  of the minimum current by Eq. (11). Both  $B$  values have already been shown in Figs. 6 and 7, respectively. In Fig. 6, both data of the  $B$ 's from Eqs. (1) and (11) appear constant against the  $\text{Ni}^{2+}$  ionic concentration, being in good agreement with each other within experimental errors.

The dependence of  $B$  in Eq. (11) on the NaCl concentration, as well as  $B$  in Eq. (1), has already been shown in Fig. 7, i.e., as mentioned before, the  $B$  value from Eq. (11) also increases with NaCl concentration. From these results, it is concluded that the  $B$  value obtained from the minimum current in Eq. (1) is the same as that from the unstable component of the minimum current in Eq. (11).

As mentioned in the previous section, the  $B$  value must be a function of  $\theta$ . Therefore, using the relationship between  $\theta$  and the NaCl concentration obtained in part II,<sup>9</sup> we replotted

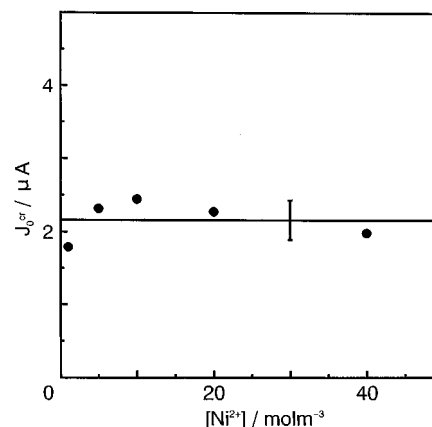


FIG. 10. Dependence of the critical unstable current,  $J_0^{\text{cr}}$  on  $\text{Ni}^{2+}$  ionic concentration.  $[\text{NaCl}] = 1000 \text{ mol m}^{-3}$ , and  $T = 300$  K.

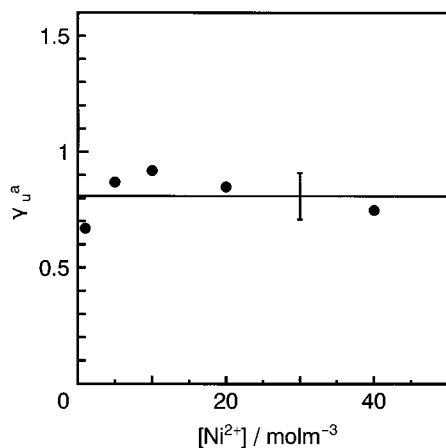


FIG. 11. Dependence of the instability ratio,  $\gamma_u^a$ , on  $\text{Ni}^{2+}$  ionic concentration.  $[\text{NaCl}] = 1000 \text{ mol m}^{-3}$ , and  $T = 300 \text{ K}$ .

ted both data shown in Fig. 7; First, the  $\theta$  was determined by the NaCl concentration, then the corresponding  $B$  value was plotted against  $1 - \theta$ . Figure 12 shows the results obtained from the data in Fig. 7, which exhibits a good linear relation. The experimental equation is, thus, given as

$$B = 3.6 + 7.4(1 - \theta) \text{ V}^{-1/2}. \quad (14)$$

That is, the coefficient  $B$  is concluded as a linear function of  $1 - \theta$ .

Therefore, as mentioned in part I,<sup>7</sup> the autocorrelation distance for the asymmetrical nonequilibrium fluctuation is experimentally determined as

$$a = (1 - \theta) \tilde{a}_{\text{cr}} \exp(-B|\langle \Phi_0 \rangle|^{1/2}), \quad (15)$$

where

$$B = B_1 + \alpha_0(1 - \theta), \quad (16)$$

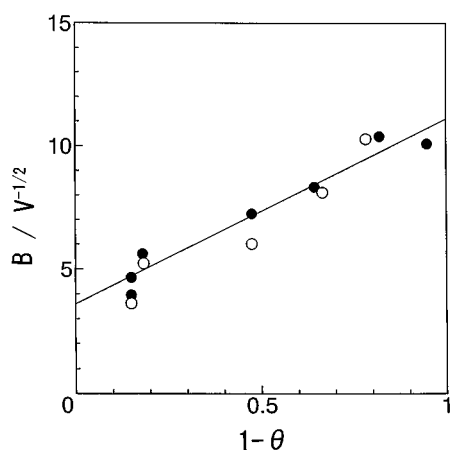


FIG. 12. Linear plot of  $B$  values given by the minimum current  $J_{\text{min}}$  and the unstable component  $J_0$  of the minimum current vs active area ratio  $1 - \theta$ .  $[\text{NiCl}_2] = 0.1 \text{ mol m}^{-3}$ , and  $T = 300 \text{ K}$ .  $\bullet$ ;  $B$  from  $J_{\text{min}}$ , and  $\circ$ ;  $B$  from  $J_0$ .

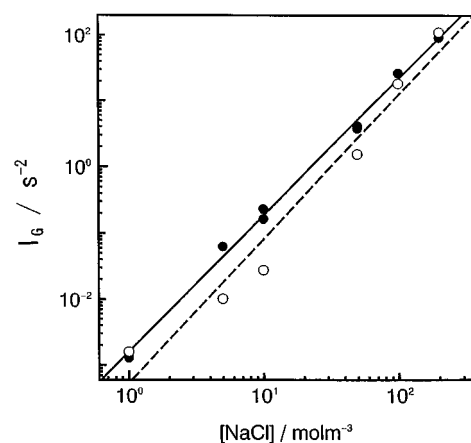


FIG. 13. Dependence of the growth factor  $l_G$  of the pitting current on NaCl concentration  $\bullet$ ; experimental data, and  $\circ$ ; theoretical data.  $V = 0.4 \text{ V}$ ,  $[\text{NiCl}_2] = 0.1 \text{ mol m}^{-3}$ , and  $T = 300 \text{ K}$ .

and  $\langle \Phi_0 \rangle$  is the total double-layer overpotential measured from the critical potential; in the present case,  $\langle \Phi_0 \rangle \approx V$ .  $B_1$  and  $\alpha_0$  are constants. From Eq. (14), they are also experimentally determined as

$$B_1 = 3.6 \text{ V}^{-1/2}, \quad (17)$$

$$\alpha_0 = 7.4 \text{ V}^{-1/2}. \quad (18)$$

From the data of the silver nucleation,<sup>10</sup> it is predicted that  $B$ , and  $\alpha_0$ , as well as  $\tilde{a}_{\text{cr}}$ , also have a generality independent of the sorts of reactions. Namely, in the silver nucleation,  $B = 13.6 \pm 1.3 \text{ V}^{-1/2}$  when the completely active surface is obtained, which is, within experimental errors, approximately agreeable with the value  $11.0 \text{ V}^{-1/2}$  derived from substituting  $\theta = 0$  into Eq. (16) with Eqs. (17) and (18).

Then, in order to examine the dependence of the coefficient  $l_G$  of the growth current on the NaCl concentration, various  $l_G$ 's were measured at constant overpotential  $V = 0.4 \text{ V}$ ; the solid circles in Fig. 13 indicate the data of the log-log plot of  $l_G$  versus NaCl concentration, which yields a linear relation with the slope of 2.06, i.e.,  $l_G$  is proportional to the second order of the NaCl concentration. Here,  $l_G$  in Eq. (9) is apparently in proportion to the first order of the NaCl concentration.

However, it is obvious from the above discussion that in the exponential part of  $l_G$  in Eq. (9), the coefficient  $B$ , as shown in Eq. (16), is a function of  $\theta$ . The  $\theta$  is, in turn, a function of the NaCl concentration as shown in part II,<sup>9</sup> so that the apparent discrepancy mentioned above may be attributed to the effect of NaCl on the  $B$  value. Including the contribution of NaCl, we reckoned  $l_G$  by Eq. (9), and again plotted the data in open circles in Fig. 13. The data replotted, as shown in Fig. 13, give an almost straight line with the slope of 2.18. Hence, it can be said that the theoretical equation Eq. (9) correctly depicts the experimental results.

Moreover, we examined how the  $l_G$  changes with the overpotential and  $\text{Ni}^{2+}$  ionic concentration; under the condition of  $1000 \text{ mol m}^{-3}$  NaCl concentration, the growth current was measured at various  $\text{Ni}^{2+}$  ionic concentrations and over-

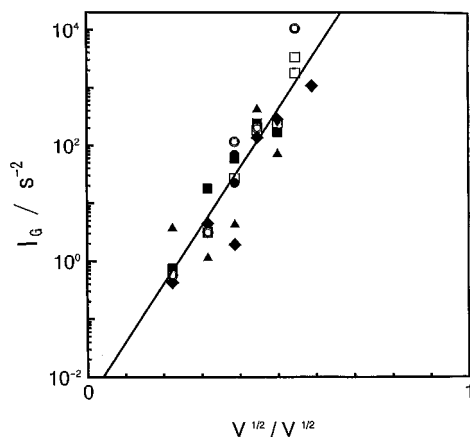


FIG. 14. Semilog plot of the growth factor,  $l_G$  of the pitting current vs  $V^{1/2}$ . ●;  $[\text{NiCl}_2]=1 \text{ mol m}^{-3}$  ■;  $[\text{NiCl}_2]=5 \text{ mol m}^{-3}$  ◆;  $[\text{NiCl}_2]=10 \text{ mol m}^{-3}$  ▲;  $[\text{NiCl}_2]=50 \text{ mol m}^{-3}$  ⊙;  $[\text{NiCl}_2]=100 \text{ mol m}^{-3}$  □; and  $[\text{NiCl}_2]=200 \text{ mol m}^{-3}$ .  $[\text{NaCl}]=1000 \text{ mol m}^{-3}$ , and  $T = 300 \text{ K}$ .

potentials. According to Eq. (9), as to the overpotentials,  $l_G$  can be expressed mainly by the exponential part as follows:

$$l_G \propto \exp(2B|V|^{1/2}). \quad (19)$$

From Eq. (19), it is expected that the semilog plot of  $l_G$  versus  $|V|^{1/2}$  yields a straight line, which is indifferent of the  $\text{Ni}^{2+}$  ionic concentration since there is no dependence of  $l_G$  on the  $\text{Ni}^{2+}$  ionic concentration as shown in Eq. (9). The individual data point in Fig. 14, as expected, forms a straight line. The linear regression of the data gives

$$\log l_G = -5.54 + 23.1V^{1/2}. \quad (20)$$

Recalling that the  $B$  value in Eq. (20) is, as shown in Fig. 7, a function of  $\theta$  and that a sufficiently high NaCl concentration like the present case, as shown in part II,<sup>9</sup> allows  $\theta$  to be zero, we can calculate the slope of the plot of  $l_G$  versus  $|V|^{1/2}$  by using Eqs. (16)–(18), i.e.,

$$2B = 22.0 \text{ V}^{-1/2}. \quad (21)$$

This shows good agreement with the observed value 23.1  $\text{V}^{-1/2}$  in Eq. (20).

#### IV. CONCLUSIONS

For pitting dissolution of nickel in a solution containing  $\text{NiCl}_2$  and NaCl, the critical autocorrelation distance of the asymmetrical fluctuations on the completely active surface was obtained, i.e.,

$$\tilde{a}_{\text{cr}} = 1.02 \pm 0.21 \text{ mm at } 300 \text{ K}.$$

This value almost agrees with that of silver nucleation within experimental errors. Therefore,  $\tilde{a}_{\text{cr}}$  is thought to have generality based on the fact that the fluctuations arise from the general nature of the thermal motion of the solution particles.

Then, in terms of the total double-layer overpotential  $\langle \Phi_0 \rangle$  and the coverage  $\theta$  of the passive film, the function form of the autocorrelation distance  $a$  was experimentally determined as follows:

$$a = (1 - \theta)\tilde{a}_{\text{cr}} \exp(-B|\langle \Phi_0 \rangle|^{1/2}),$$

$$B = B_1 + \alpha_0(1 - \theta),$$

where  $B_1$  and  $\alpha_0$  are also constants, being decided as  $B_1 = 3.6 \text{ V}^{-1/2}$  and  $\alpha_0 = 7.4 \text{ V}^{-1/2}$ . As discussed in part II, since  $\theta$  is a function of NaCl concentration,  $a$  and  $B$  change with NaCl concentration.

When the nonequilibrium fluctuations turn unstable, the pitting dissolution is activated to increase the pit-growth current. However, all the fluctuations do not develop, i.e., about 80% of them become unstable. Then, the equation of the pit-growth current is written as

$$J = J_0 \exp(l_G t^2),$$

where the growth factor  $l_G$  is a function of the NaCl concentration and the applied overpotential, but not of the  $\text{Ni}^{2+}$  ionic concentration. Namely,  $l_G$  is in proportion to the second order of NaCl concentration and the exponential of  $|V|^{1/2}$ .

#### ACKNOWLEDGMENT

The authors thank Mr. Eiji Yamamoto at the Polytechnic Center Shiga for providing experimental data and stimulating, fruitful, and enjoyable discussions.

<sup>1</sup>N. Sato, J. Electrochem. Soc. **129**, 260 (1982).

<sup>2</sup>T. Yoshii and Y. Hisamatsu, J. Jpn. Inst. Met. **35**, 151 (1971); **36**, 750 (1972).

<sup>3</sup>S. Tsujikawa, in Proceedings of the 7th Corrosion Seminar, Japan Society of Corrosion Engineering, Tokyo, 1980, p. 1.

<sup>4</sup>Y. Hisamatsu, in Passivity and Its Breakdown on Iron and Iron Base Alloys, p. 99, NACE, Houston, 1976.

<sup>5</sup>K. J. Vetter and H. H. Strehblow, Ber. Bunsenges. Phys. Chem. **74**, 1024 (1970).

<sup>6</sup>N. Sato, in Proceedings of the 2nd Japan-USSR Corrosion Seminar, p. 35, JSCE (1980).

<sup>7</sup>M. Asanuma and R. Aogaki, J. Chem. Phys. **106**, 9930 (1997), first paper of this series.

<sup>8</sup>R. Aogaki, J. Electrochem. Soc. **142**, 2964 (1995).

<sup>9</sup>M. Asanuma and R. Aogaki, J. Chem. Phys. **106**, 9938 (1997), preceding paper.

<sup>10</sup>A. Tadano and R. Aogaki, J. Chem. Phys. **106**, 6138 (1997).